Mechanical Behaviour of Two Leaves Masonry Walls Strengthening using Different Grouts

Eduarda Luso[1], Paulo B. Lourenço[2]

[1]Corresponding Author, Ph.D., ISISE, Polytechnic Institute of Bragança, Department of Civil Constructions, Campus Sta Apolónia, 5300-253 Bragança, Portugal. Phone: +351 273 30 30 70, email: eduarda@ipb.pt

[2]Professor, Ph.D., ISISE, University of Minho, Department of Civil Engineering, Azurém, 4800-058 Guimarães, Portugal. Phone: +351 253 510 209, fax: +351 253 510 217, E-mail: pbl@civil.uminho.pt

ABSTRACT

Grout injection is an efficient method to improve the mechanical characteristics of masonry walls, in the presence of voids or cracks. Masonry made up of two exterior leaves with the space between them filled with poor infill with a large amount of voids is common in many existing structures. In other cases, dry stack masonry is used. Grouting of these types of vulnerable masonry with lime based grouts was proven mechanically efficient. The success of this technique depends on several parameters, such as injection pressure, the general condition of the masonry (materials and mechanical properties) and the rheological properties of the grout. The effect of ternary grouts and hydraulic lime-based grouts on the compressive and shear strength of three-leaf stone masonry has been widely investigated. However, fewer studies have been done on walls with one or two leafs, as done in this paper.

The present research aims to investigate the mechanical performance of schist masonry walls before and after injection. Six masonry walls of typical schist stone constructions from the North of Portugal were constructed in accordance with the original construction materials and were tested under compressive load. Two different grouts were chosen to inject the wall specimens (one commercially available and another prescribed). The results obtained showed that these strengthening techniques were successful in increasing the compressive strength of the walls and in improving their behaviour under compressive loads.

Keywords: Schist masonry, grout, injection, walls

1. INTRODUTION

Schist constructions are an important cultural, architectural and historical legacy in Europe, and particularly in Portugal, whose preservation is of importance. There are many buildings in schist masonry spread all over Portugal, varying in terms of buildings typology, constructive techniques and even type of schist (Barros *et al.* 2010). Schist masonry in North-eastern Portugal typically has two types of constructions: with mortar joints, usually with mixtures based on clay or lime; or with dry joints, normally used in encircling walls, mills and shelters (see Figure 1).

Similar to other stone masonry constructions, schist masonry buildings suffer damage due to their weak tensile strength. Therefore, they frequently need stabilization, repair or strengthening. Cement and lime-based grouting is a well-known intervention technique, which can be durable and mechanically efficient whilst preserving the historical nature of the structure to a reasonable extent. Parameters such as rheology, injectability and stability of the grout mix should be considered to ensure the effectiveness of any injection. Grouting is efficient when applied to types of masonry encountering a large percentage of voids, mainly to the quite frequent type of three-leaf masonry (Vintzileou, 2006; Vintzileou & Miltiadou-Fezans, 2008). The effectiveness of the injection technique has long been directed to this type of masonry in many research works (Valluzzi, 2000; Vintzileou, 2011; Oliveira *et al*., 2012; Silva, 2013). However, in this study, the effectiveness of this technique in schist masonry walls, which traditionally have a building typology of one or two leafs, was tested. Six wall specimens with mortared joints were built. The mortar composition was chosen to be representative of the old mortar in terms of components, strength and deformability. Four walls were subsequently injected with two types of lime-based grout. One of the chosen grouts was a ready-mix commercially available grout (*Mape-Antique I* of *Mapei*), which was compared with other commercial grouts by Luso & Lourenço (2016). The second grout adopted was a composition formulated in the laboratory (Luso & Lourenço, 2017b) with similar results compared to the commercial grout, but not compared in full masonry walls. After an extended laboratory study on the two grouts (Luso & Lourenço, 2017a) the behaviour of walls injected with these products was evaluated, with the aim to increase the mechanical strength of the walls and improve their deformability.

2. EXPERIMENTAL PROGRAM

The experimental research presented in this paper involved the construction, injection and testing of three sets of schist masonry walls. All the procedures were done in the Laboratory of Structures at University of Minho, in Guimarães, Portugal. A description of the materials and the construction method used is done in the next sections.

2.1. Stone

The shale used for the construction of the walls came from Vila Nova de Foz Côa, North of Portugal. It was directly extracted from the quarry and transported on pallets to Guimarães, without any treatment. A detailed description of this stone can be found in Barros (2013). These stones break easily along their foliation planes (Barros *et al.*, 2014), when applying a stroke with a hammer and, if necessary, with a pointer and a chisel. Then, the pieces are cut according to the required shape for the wall construction, resulting in irregularly shaped stone pieces (see Figure 2). The schist, kept packed on pallets and covered with plastic and placed outside until the time of the walls construction, presented an average moisture content of 0.2%, in a test following the procedure described in EN 1097-5:2001.

2.2. Mortar

For the preparation of the mortar, a fine grain sand from a local supplier was used. As binder, hydrated lime CL90-S, from Lusical and the natural hydraulic lime NHL5 of Cimpor company, were used. The binder/sand proportion adopted was 1:2, while a water binder ratio of 0.4 (all ratios in weight). The choice of materials used was based on studies conducted by Rodrigues (2004).

The compressive strength of the mortar was assessed on prismatic specimens of $16x4x4cm^3$ and cylinders with 7cm of diameter and 14.5cm of height for the determination of the Elastic Modulus, sampled during the construction of the wall specimens and following the procedures described in the standards EN 1015-11 (1999) and ASTM C469 (2002) respectively. Similar curing conditions to those of the walls were adopted for the mortar specimens (in average 20ºC of temperature and 70% of relative humidity), which were subsequently tested under compression at the ages 28, 90 and 150 days, for the prismatic specimens. Three prismatic specimens of each age were tested, as well, for cylinders specimens (see Figure 3 (b)).

The average compressive mortar strengths computed for the aforementioned ages were 0.71MPa, 0.76MPa and 0.85MPa, respectively (see Table 1). At 150 days, compression tests were carried out both prismatic and cylindrical specimens. In specimens with cylindrical shape, vertical deformation was measured using three displacement transducers (*lvdt*) arranged at 120º and fixed to the sample (see Figure 3 (a)). The tests were performed under displacement control (5μm/s). The results are shown in the stress-strain graph for three of the samples tested (see Figure 3 (b)). On average, the mortar has a "low" compression strength (< 1 MPa). The average value of the elastic modulus is also low which for this type of mortar is compatible with the masonry wall support. The ratio between elastic modulus and compressive strength is 880, which compares well with the value defined in EN 1996-1-1 (2005) for masonry. It is noted that the deformation properties in the inelastic range present a much higher variability than the compressive strength and elastic modulus.

2.4 Walls' geometry and construction

Six walls in schist masonry were built in the Structures Laboratory of the University of Minho by the same experienced team of masons. The most common schist masonry typology (two leaves) was reproduced using traditional building techniques. The number of specimens was limited due to the size of the walls and due the space available in the laboratory for the storage of the walls for the necessary period of curing and testing, so only two replicas were built for each specimen type.

The construction of the schist walls in the laboratory took about six days, on average one wall per day. The walls were constructed on a stiff steel base, overlaying stones pieces with different sizes and with a coursed arrangement, given the weak resistance schist has in the stratification direction. A scheme and image of the wall construction are shown in Figure 4 and Figure 5(a). The overlap of the corners and the connection between leaves was duly considered, with the placement of stones in perpendicular direction in each layer, with mortar and gravel or small schist pieces. A void volume within the masonry was ensured, to allow the grouting process, and in addition, represent a typical schist masonry wall. An identical stiff steel plate of the base was placed on top after completion of construction to slightly pre-compress the walls along the vertical direction in order to simulate real conditions and to minimize any possible damage caused by drilling or injection pressure.

The wall specimens are 0.70m wide, 0.89m high and 0.45m thick. The final aspect of one of the walls can be seen in Figure 5 (b). For details on the construction sequence, height of courses, average thickness of horizontal joints and geometrical details of the walls, see Luso (2012). The walls remained in place after construction for ten weeks curing and then the grouting work began.

2.5 Hydraulic grouts

Many commercial ready-mix grouts are available in the market and have been frequently prescribed by designers or proposed by specialized contractors. The behaviour of four commercial grouts under laboratory conditions was recently evaluated (Luso & Lourenço, 2016). However, the use of cement and lime-based grouts formulated in the laboratory with the addition of other materials such as fly ashes, silica fume, bentonite, hydraulic lime, among others, are proposed by different researchers (Binda *et al.,* 1992; Perret, 2002; Toumbakari, 2002; Miltiadou-Fezans *et al.,* 2006; Vintzileou, 2006; Kalagri *et al.,* 2010; Papayianni & Pachta, 2014). The use of calcined clay, in the form of metakaolin, as a pozzolanic material for mortars and concretes has received considerable attention in recent years and constitutes also a good option (Sepulcre-Aguilar & Hernandez-Olivares, 2010; Brooks & Johari, 2001, Melo & Carneiro, 2010; Billong *et al.*, 2009; Cachim *et al.,* 2010; Lee *et al.,* 2005; Gleize *et al.* 2007).

A composition with metakaolin, white cement and hydrated lime, mixed with a plasticizer show satisfactory mechanical and physical properties, which is a viable alternative to the commercial grouts available, either due to cost, availability or technical considerations (Luso & Lourenço, 2017). Therefore, two grouts were chosen for the injection of the walls: *Grout A* is a hydraulic grout developed by *Mapei* – Italy, for historical masonry (Mape-Antique I); *Grout B* is a hydraulic grout prescribed with 30% of white cement CEM II B/L-32,5R from (*Secil* – Portugal), 30% of hydrated lime type CL90 from *Baptistas* – Portugal, 35% of metakaolin Optipozz-sc, water/binder ratio equal 0.6 and superplasticizer (Dynamon SR1 from Mapei). Table 2 shows some of the main properties obtained for the grouts (Luso & Lourenço, 2016; Luso & Lourenço, 2017).

2.6 Preparation of walls for Grout Injection

The walls were prepared for grouting followed well-established procedures (Miltiadou-Fezans *et al.*, 2005; Silva, 2008; Biçer-Simsir & Rainer, 2013). A series of injection holes have been drilled on one side, slightly inclined downwards and with a depth of 20-25cm, following a scheme approximately of equilateral triangles. Into each hole, plastic tubes with 8mm diameter were introduced and sealed with silicone. All tubes were numbered for better control of the injection process. In the day before the injection process, water was injected in order to wet the interior of each wall and avoid excessive water absorption during grouting.

2.7 Grout Injection

Once the walls had been prepared, the grout was introduced at low pressure (around 1.5bar) in the interior using a pressure pot, starting from the bottom up to the top of the wall.

The grouts were mixed using a mechanical device of low turbulence for about 10 minutes. Each type of grout was injected into two walls (*P2* and *P6* with *Grout A*, *P1* and *P3* with *Grout B*), (see Figure 6). Hereafter, the walls are designated as *P4 nI* and *P5 nI*, for the walls not injected, *P2 IA* and *P6 IA* for the walls injected with *grout A* and finally *P1 IB* and *P3 IB* for the walls injected with *grout B*. During the injection procedure the active and inactive holes were identify, as well as the volume of grout introduced, the appearance of cracks or not, and the quantity of grout lost in leaks. On average, $50dm^3$ and $42.5dm^3$ of *grout A* and *grout B* respectively were injected per wall (grout leakage was negligible), corresponding to a volume of 12%, on average, of the total volume specified for the walls. Additional details on the procedure can be found in Luso (2012).

3. TESTING SETUP AND MEASUREMENTS

All wall specimens were tested under monotonic compression using a 2MN closed-loop servo-controlled testing machine (see Figure 7). The tests were performed under displacement control at a constant rate of 5 μm/s. During the tests, the displacements in the walls were measured by means of linear variable displacement transducers (lvdt´s) disposed according to Figure 8. The lvdt layout in the walls aimed at measuring vertical, horizontal and transversal displacements directly on the walls, in order to compute mechanical parameters. One external lvdt (lvdt, v5) was used to measure the displacement between the plates of the testing machine and to control the tests.

In the case of the walls strengthened by injection (*P1, P2, P3* and *P6*), the external leaves were carefully dismantled after testing, in order to check the quality of the strengthening procedure.

4. RESULTS AND DISCUSSION

4.1. Experimental results for non-injected masonry walls *P4 nI* and *P5 nI*

Table 3 summarizes the results of the compressive tests carried out on the two unstrengthened walls *P4 nI* and *P5 nI*, in terms of compressive strength ($f_{c,w}$), vertical strain ($\varepsilon_{v,p}$) and horizontal strain ($\varepsilon_{h,p}$) at peak load, Young´s modulus computed in the [0%-20%], stress range (E_0) and in the [30%-60%] stress range (E_{30-60}), and Poisson's ratio in the [30%-60%] stress range (ν_{30-60}).

Taking into account the heterogeneity presented by the masonry of the tested walls, due to the dimensions and irregular geometry of the stones, as well as the variable number and thickness of joints, a high dispersion of the results would be expected. However, there are only significant differences between the two walls for the strains, $\varepsilon_{v,p}$ and especially for $\varepsilon_{h,p}$, while for the rest of the parameters similar results were found

In Figure 9, the good approximation between the displacements verified in the internal scheme (average of values obtained in lvdt, v1 and v2, see Figure 7) and in the external scheme (lvdt, v5) can be seen in face B, for walls *P4 nI* and *P5 nI*. There is some difference between measurements on face B and face D, as usual in this type of tests due to inevitable rotation, or non-symmetric failure, of the specimen in the post-peak regimen. Figure 10 shows the variation of the angle of rotation with the stress level installed.

In relation to the horizontal deformation recorded on the transverse faces A and C, (see Figure 11), values of the same order of magnitude were observed in both walls (face B and D), (see Figure 12), since the number of joints in the measuring field is identical (at most, one or two joints between the lvdt's). The graphs of Figure 11 show that the transverse deformation occurs, fundamentally, and abruptly, at load values close to the peak load and increases significantly after rupture. These results are similar to most failures of single leafs masonry walls, which occur in the transverse direction.

4.2. Experimental results for injected masonry walls

The results concerning injected walls *P1, P2, P3* and *P6* are summarized in Table 4 and Table 5. The parameters were determined from the analysis of the results obtained in the uniaxial compression tests. The average value of the compressive strength obtained was about three times higher than the average value obtained for the non-reinforced walls, for both *grout A* and *grout B*.

The obtained elastic modulus (E_0 and $E_{[30\text{-}60\%]}$) also have values, on average, higher than those obtained for non-reinforced walls. In addition, the value of modulus of elasticity E_0 is also greater than $E_{[30\text{-}60\%]}$. Among the reinforced walls, *P1 IB* and *P3 IB* presented similar values for the modulus of elasticity and the compressive strength. The walls reinforced with *grout A* presented a high dispersion, both for the modulus of elasticity and for the tensile strength. This is due to the differences in the walls, in particular the different thickness and quantity of joints, the number of stone courses and the high irregularity of the masonry, among others. In the injection of these two walls there was a significant difference in the quantity of injected grout (42 litres in *P6* and 23 litres in *P2*), which indicates a larger volume of voids in wall *P6*, so it is likely that the quantity of stone in wall *P2* is quite higher than *P6*.

In the stress-vertical strain graphs of Figure 13 it can be verified that there is no significant difference between the vertical displacements in the internal scheme (average of values obtained in lvdt, v1 and v2) and in the external scheme (lvdt, v5) in face B for walls *P1 IB* and *P6 IA*. However, in the walls *P3 IB* and *P2 IA* there was some difference, (see Figure 14). In these two walls, the curvature of the graph at the initial phase of the test shows a more pronounced concavity associated with some adjustment of the steel plates to the test wall specimen. Comparing the measurements on face B and face D with respect to the vertical deformation, an increase in wall rotation from about 60% of the maximum load is observed on wall *P3 IB*. The evolution of the rotation of the strengthened walls with the applied stress level can be seen in Figure 15 and Figure 16.

Regarding the horizontal deformation, the deformations of the transverse faces A and C, (see Figure 17 and Figure 18), are similar to those of faces B and D, (see Figure 19 and Figure 20).

4.3. Comparison of results

Following the analysis of the results of each wall, Figure 21 shows the vertical stress-strain diagrams for the six walls tested, with and without grouting, in order to facilitate comparison. In Table 6, the average values obtained in each type of strengthened wall are compared with the mean values obtained on the unstrengthened walls. It is found that the injection has significantly increased the compressive strength of the walls (about three times), and also the stiffness of the walls, about five times. The two grouts seem to have performed similarly in terms of strength and initial stiffness.

The appearance of the first horizontal and vertical cracks, as well as the respective applied load, is given in Figure 22 and Figure 23, respectively. On average, the first horizontal cracks appear at about 50% of the maximum load, while vertical cracks arise at about 80% of the maximum load. The crack initiation was defined by the lvdts and is rather objective, corresponding to a significant increase of measurements.

Several compression tests on masonry walls, in order to evaluate the injection technique effectiveness, were conducted over the past few years. It is therefore inevitable to compare these results with the results of the experimental campaign presented here (Valluzzi, 2000; Valluzzi *et al.*, 2001; Valluzzi *et al.*, 2004; Vintzileou, 2007; Silva, 2008; Silva *et al*., 2014 Almeida *et al.,* 2012; Toumbakari, 2002; Miltiadou- Fezans *et al*., 2006). A summary of these results is show in Table 7.

A common result is that the injection increases the load capacity and stiffness of the walls. The direct comparison of the remaining values is risky because the procedures and test schemes are different from work to work, with multiple aspects that influence the results obtained. In addition, the walls tested in this work present a different constructive typology of the walls of three leaf often used in previous works. Also, the analytical models presented in literature studies to estimate the compressive strength were formulated for three-leaf masonry walls (Egermann *et al.,* 1994; Vintizielou and Tassios, 1995; Pina-Henriques, 2005; Vintzileou & Miltaidou-Fezans, 2008), considering the geometrical characteristics of the walls, namely width of the leafs and the compressive strength of the exterior and interior leaf. These models are not for the type of masonry presented in this paper. The Italian regulation (OPCM, 2005) recommends to increase the mechanical characteristics through injection to the double, which the present work confirms as conservative, meaning that it can be adequate for practical purposes.

5. CONCLUSIONS

This paper addresses the use of grout in single leaf walls made of shale stone from the north of Portugal and a lime based mortar. The typological and geometrical characteristics of the walls were tested is also described, as well as the mechanical properties of the mortar. Two of the built walls were not strengthened and the remaining four walls were strengthened with two different grouts. One grout was commercially available grout from Mapei company and another grout was prescribed in the laboratory. The injection process was very similar with a good injectability for both grouts. The consumption of the prescribed grout in the injection of the two walls was similar. In the case of the commercially grout, the quantity injected in the two walls was different, due to the typology of the specimen, which led to some dispersion of the results.

Finally, the results of the uniaxial compression tests carried out on the walls, not strengthened and strengthened with injection, were discussed in this paper. These tests took place 90 days after the injection and allowed to evaluate the influence of this strengthening technique on the behaviour of this typology of walls under vertical actions. It should be noted that: (i) the injection technique has led to an increase in compressive strength of three times, and an increase to the modulus of elasticity of five times; (ii) the applied strengthening technique did not lead to a significant difference in strains corresponding to the maximum stress, thus increasing the brittleness of the response.

6. REFERENCES

Almeida, C., Guedes, J. P., Arêde, A., Costa, C. Q., & Costa, A. (2012). Physical characterization and compression tests of one leaf stone masonry walls. *Construction and Building Materials*, *30*, 188-197.

ASTM C469 (2002). Standard Test Method for Static Modulus of Elasticity and Poisson´s Ratio of Concrete in compression. Developed by Subcommittee: C09.61

Barros, R. (2013). Avaliação do comportamento material e estrutural de construções em xisto. PhD Thesis, University of Minho (in Portuguese)

Barros, R. S., Oliveira, D. V., & Varum, H., (2010). Typological characterization of the Portuguese traditional schist constructions. 37th IAHS World Congress on Housing Science: design, technology, refurbishment and management of buildings, http://hdl.handle.net/10773/7766

Barros, R. S., Oliveira, D. V., Varum, H., Alves, C. A., & Camões, A. (2014). Experimental characterization of physical and mechanical properties of schist from Portugal. *Construction and Building Materials*, *50*, 617-630.

Biçer-Simsir, B., & Rainer, L. (2011). Evaluation of lime-based hydraulic injection grouts for the conservation of architectural surfaces. *A Manual of Laboratory and Field Test Methods, GCI*.

Billong, N., Melo, U. C., Njopwouo, D., Louvet, F., & Bonnet, J. P. (2009). Effect of mixture constituents on properties of slaked lime–metakaolin–sand mortars containing sodium hydroxide. *Cement and concrete composites*, *31*(9), 658-662.

Binda, L.; Baronio, G.; Squarcina, T. (1992): *Evaluation of the durability of bricks and stones and of preservation treatments*, Proceedings of the 7th International Congress on Deterioration and Conservation of Stone: held in Lisbon, LNEC, Portugal

Brooks, J. J., & Johari, M. M. (2001). Effect of metakaolin on creep and shrinkage of concrete. *Cement and Concrete Composites*, *23*(6), 495-502.

Cachim, P., Velosa, A. L., & Rocha, F. (2010). Effect of Portuguese metakaolin on hydraulic lime concrete using different curing conditions. *Construction and building materials*, *24*(1), 71-78.

Egermann, R., & Newald-Burg, C. (1994). Assessment of the load bearing capacity of historic multiple leaf masonry walls. In *Proceedings of the 10th international brick block masonry conference* (pp. 1603-1612).

EN 1015-11 (1999). Methods of test for mortar for masonry Part 11: Determination of flexural and compressive strength of hardened mortar.

EN 1097-5 (2001). Tests for mechanical and physical properties of aggregates. Determination of water content by drying in a ventilated oven.

EN 1996-1-1 (2005). Eurocode 6. Design of masonry structures; Part 1-1: General rules for reinforced and unreinforced masonry structures. CEN/TC 250 – Structural Eurocodes

Gleize, P. J., Cyr, M., & Escadeillas, G. (2007). Effects of metakaolin on autogenous shrinkage of cement pastes. *Cement and Concrete composites*, *29*(2), 80-87.

Kalagri, A., Miltiadou-Fezans, A., & Vintzileou, E. (2010). Design and evaluation of hydraulic lime grouts for the strengthening of stone masonry historic structures. *Materials and structures*, *43*(8), 1135-1146.

Lee, S. T., Moon, H. Y., Hooton, R. D., & Kim, J. P. (2005). Effect of solution concentrations and replacement levels of metakaolin on the resistance of mortars exposed to magnesium sulphate solutions. *Cement and concrete research*, *35*(7), 1314-1323.

Luso, E. (2012) *Experimental analysis of lime based grouts for the ancient masonry injections,* PhD Thesis, University of Minho, Portugal. Available from http://hdl.handle.net/1822/23073

Luso, E., & Lourenço, P. B. (2016). Experimental characterization of commercial lime based grouts for stone masonry consolidation. *Construction and Building Materials*, *102*, 216-225.

Luso, E., & Lourenço, P. B. (2017) a). Experimental laboratory design of lime based grouts for masonry consolidation. *International Journal of Architectural Heritage*, *11*(8), 1143-1152.

Luso, E., & Lourenço, P. B. (2017) b). Bond strength characterization of commercially available grouts for masonry. *Construction and Building Materials*, *144*, 317-326.

Melo, K. A., & Carneiro, A. M. (2010). Effect of Metakaolin's finesses and content in self-consolidating concrete. *Construction and Building Materials*, *24*(8), 1529-1535.

Miltiadou-Fezans, A., Papakonstantinou, E., Zambas, K., Panou, A., & Frantzikinaki, K. (2005). Design and application of hydraulic grouts of high injectability for the structural restoration of the column drums of the Parthenon Opisthodomos. *Transactions on the built environment*, 461-471.

Miltiadou-Fezans, A.; Vintzileou, E.; Papadopoulou, E.; Kalagri, A. (2006): *Mechanical Properties of Three-Leaf stone Masonry afther Grouting*, Structural Analysis of Historical Constructions, Lourenço P. B., Roca P., Modena C., Agrawal S. (eds), New Delhi

Oliveira, D. V., Silva, R. A., Garbin, E., & Lourenço, P. B. (2012). Strengthening of three-leaf stone masonry walls: an experimental research. *Materials and structures*, *45*(8), 1259-1276.

OPCM, Ordinanza 3474-3431 (2005): *Norme tecniche per il progetto, la valutazione l'adeguamento sismico degli edifici*

Papayianni, I., & Pachta, V. (2015). Experimental study on the performance of lime-based grouts used in consolidating historic masonries. *Materials and structures*, *48*(7), 2111-2121.

Perret, S. (2002): *Rôle du degré de saturation dês sables fins à moyens sur leur injectabilité par dês coulis de ciment microfin*, Thèse de Doctorat ès Sciences appliquées, Spécialité: Génie civil, Université de Sherbrooke (Québec) Canada

Pina-Henriques J. (2005): *Masonry Under Compression: Failure Analysis and Long- Term Effects*, PhD dissertation, Universidade do Minho, Guimarães

Rodrigues, M. P. (2004): *Argamassas de Revestimento para Alvenarias Antigas. Contribuição para o estudo da influência dos ligantes*, PhD Tese, UNL, Lisboa

Sepulcre-Aguilar, A., & Hernández-Olivares, F. (2010). Assessment of phase formation in lime-based mortars with added metakaolin, Portland cement and sepiolite, for grouting of historic masonry. *Cement and Concrete Research*, *40*(1), 66-76.

Silva, B., Pigouni, A. E., Valluzzi, M. R., & Modena, C. (2014). Calibration of analytical formulations predicting compressive strength in consolidated three-leaf masonry walls. *Construction and Building Materials*, *64*, 28-38.

Silva, R. (2008) *Experimental characterization of masonry: strengthening and long term effects*, Master Thesis, University of Minho (in Portuguese), Portugal. Available from http://hdl.handle.net/1822/9036

Toumbakari, E. (2002): *Lime-Pozzolan-Cement Grouts and their Strutural Effects on Composite Masonry Walls,* PhD Thesis, Department of Civil Engineering, Katholieke Universiteit Leuven, Belgium.

Valluzi, M. (2000): *Comportamento Meccanico di Murature Consolidate Con Materiali e Tecniche a Base di Calce*, Tesi de Dottorato, Universita Degli Studi di Trieste.

Valluzi, M.; da Porto, F.; Modena C. (2001): *Behaviour of multi-leaf stone masonry walls strengthened by different intervention techniques*, Historical Constructions, Lourenço P. B. and Roca P. (eds), Guimarães

Valluzzi, M. R., Da Porto, F., & Modena, C. (2004). Behavior and modeling of strengthened three-leaf stone masonry walls. *Materials and structures*, *37*(3), 184-192.

Vintzileou, E. (2006): *Grouting of Three-Leaf Stone Masonry: Types of Grouts, Mechanical Properties of Masonry before and after Grouting*, Structural Analysis of Historical Constructions, Lourenço P. B., Roca P., Modena C., Agrawal S. (eds), New Delhi.

Vintzileou, E. (2007). Iniezione di miscela fluida in muratura a sacco: Risultati sperimentali e previsione delle caratteristiche meccaniche. In *Seminar CIAS Evoluzione nella sperimentazione per le costruzioni* (pp. 191-211).

Vintzileou, E. (2011) *Three-leaf stone masonry in compression, before and after grouting: A review of literature*. International Journal of Architectural Heritage, 5: 513-538, Taylor & Francis

Vintzileou, E., & Miltiadou-Fezans, A. (2008). Mechanical properties of three-leaf stone masonry grouted with ternary or hydraulic lime-based grouts. *Engineering Structures*, *30*(8), 2265-2276.

Vintzileou, E.; Tassios, T. (1995): *Three-Leaf Stone Masonry Strengthened by Injecting Cement Grouts*, Journal of Structural Engineering, Vol. 121 (5): 848-856.

FIGURES

Figure 1 – Schist masonry walls: (a) and (b) with mortar joints; (c) with dry joints

Figure 2 - Appearance of schist stones after cutting with hammer and pointer

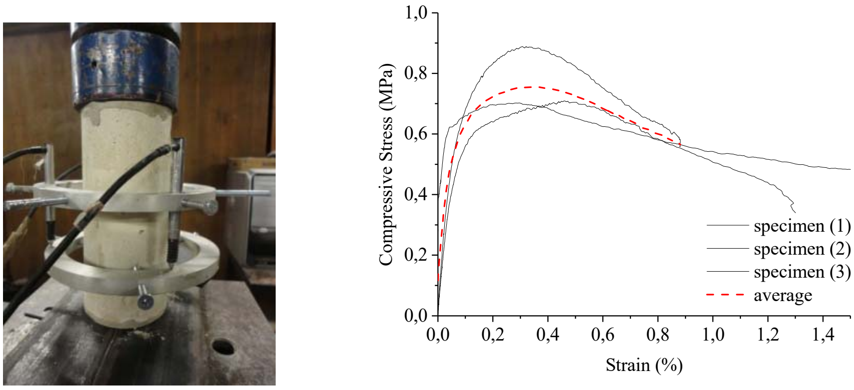

(a) (b)

Figure 3 – (a) Compression test; (b) Stress-strain graph obtained in compression test

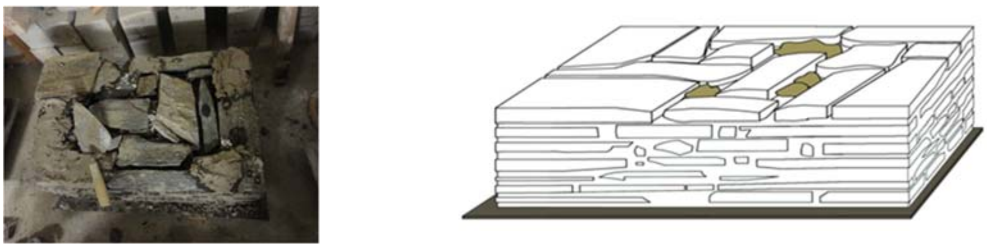

Figure 4 – Construction of the walls

Figure 5 – (a) Construction of the walls (b) Final aspect of the wallet P4

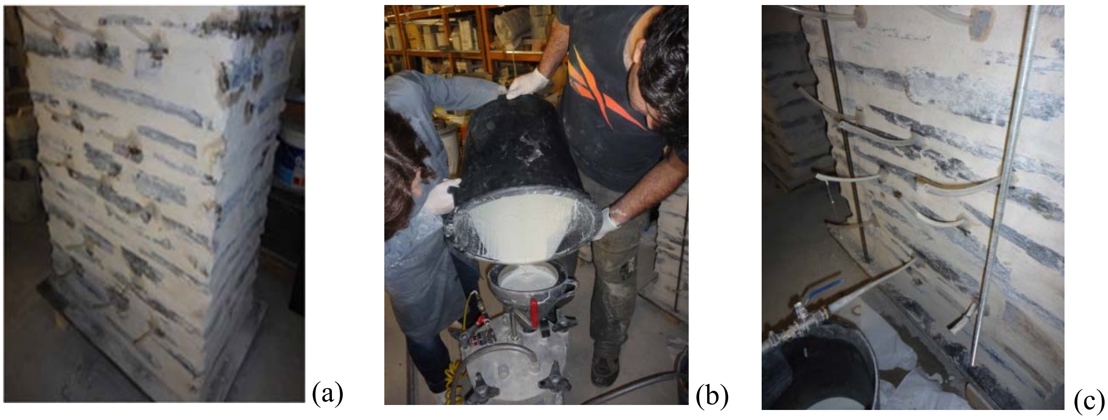

Figure 6 – (a) Wallet final aspect before grouting; (b) Introduction of grout in the pressure pot; (c) Injection of the walls

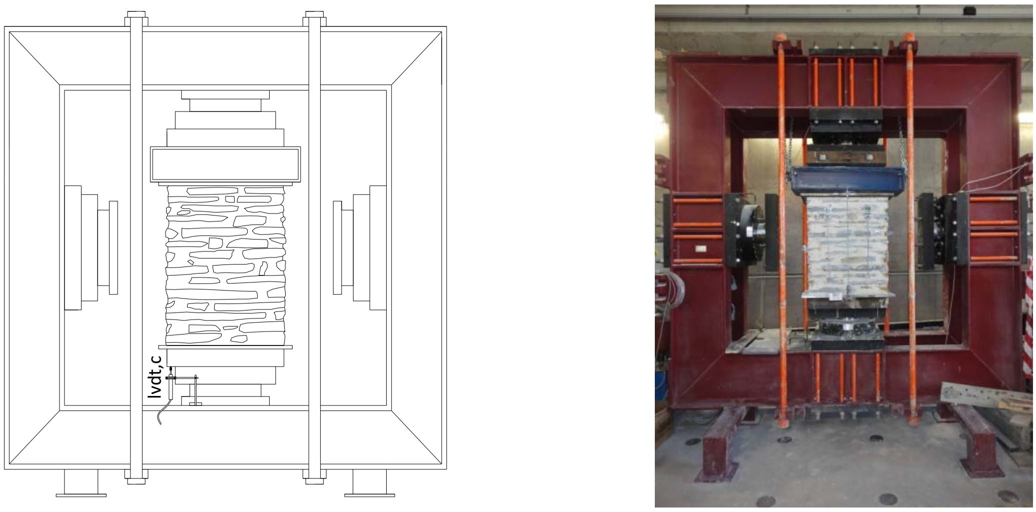

Figure 7 – Test setup of the walls: scheme and testing machine

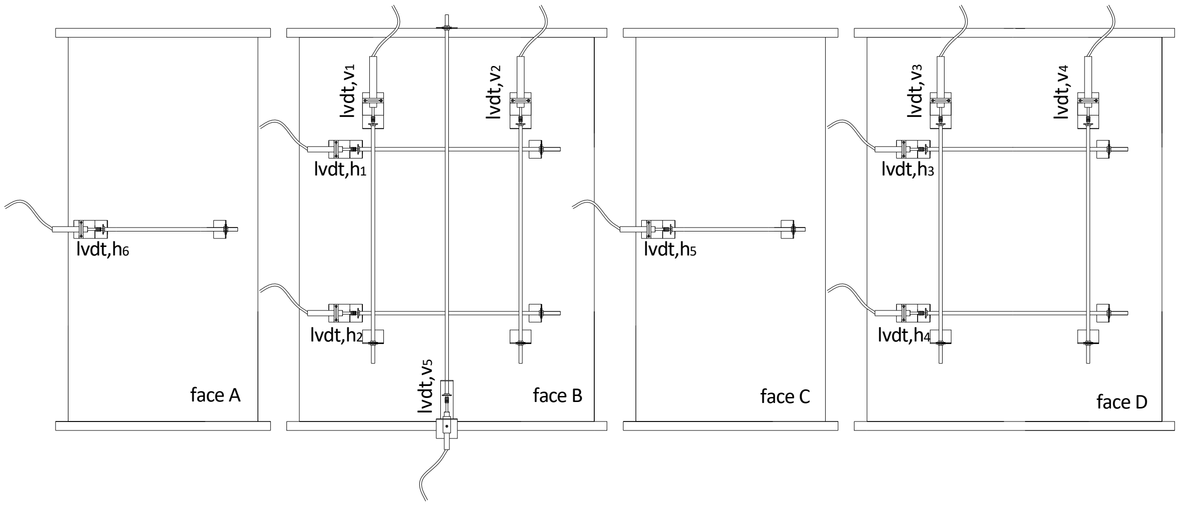

Figure 8 – Test setup of the walls: location of the displacement transducers (faces a, b, c and d are, respectively, left, front, right and back with respect to Figure 7

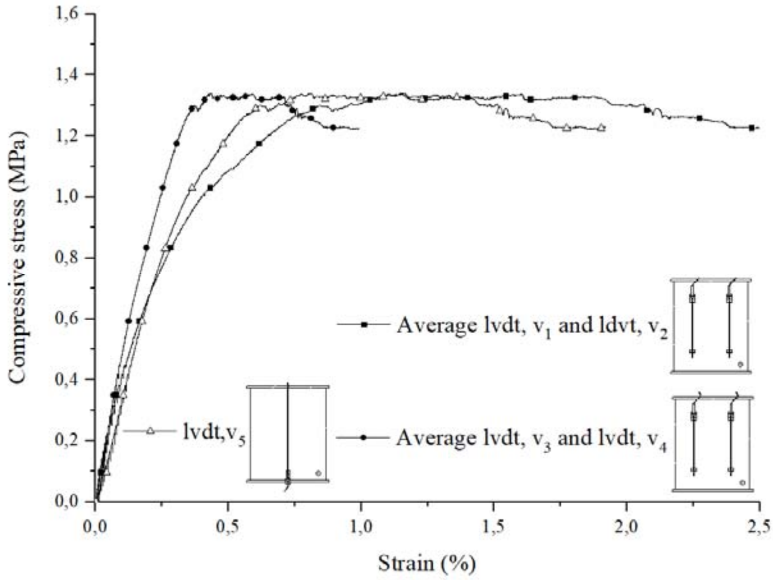

(a)

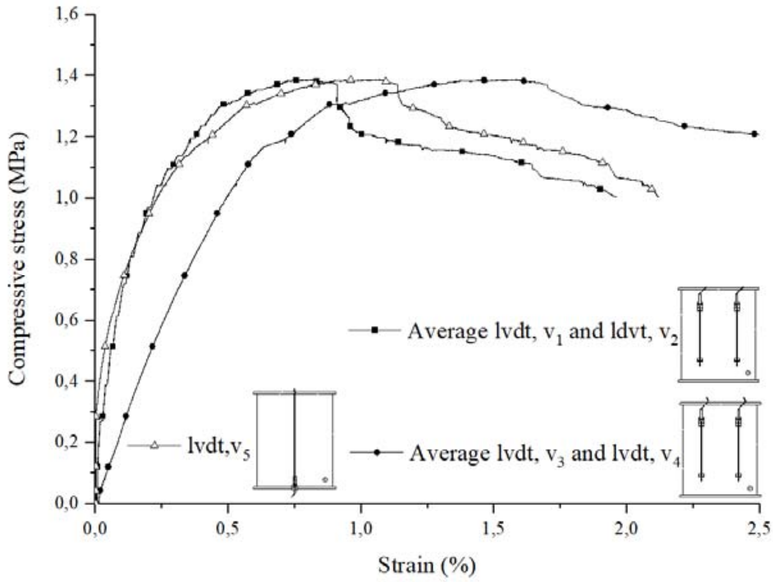

(b)

Figure 9 – Relation between compressive stress-vertical extension in: (a) *P4 nI* and (b) *P5 nI*

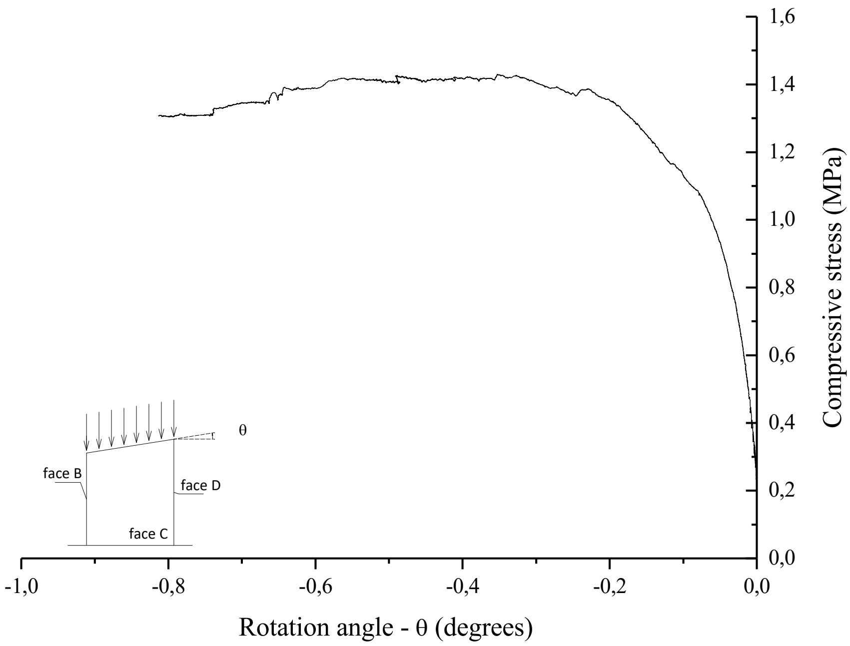

(a)

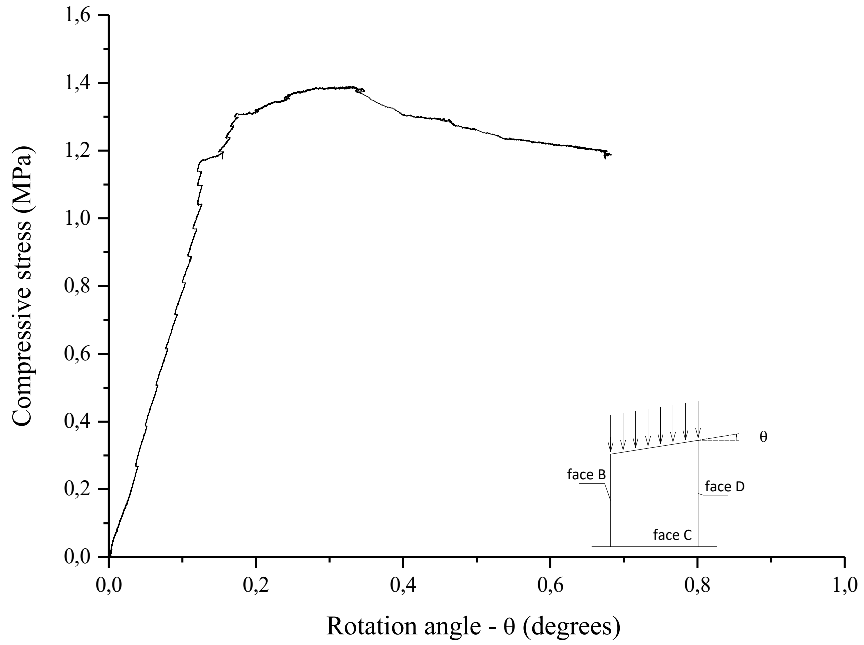

(b)

Figure 10 – Compressive stress vs angle of rotation of the walls: (a) *P4 nI;* (b) *P5 nI*

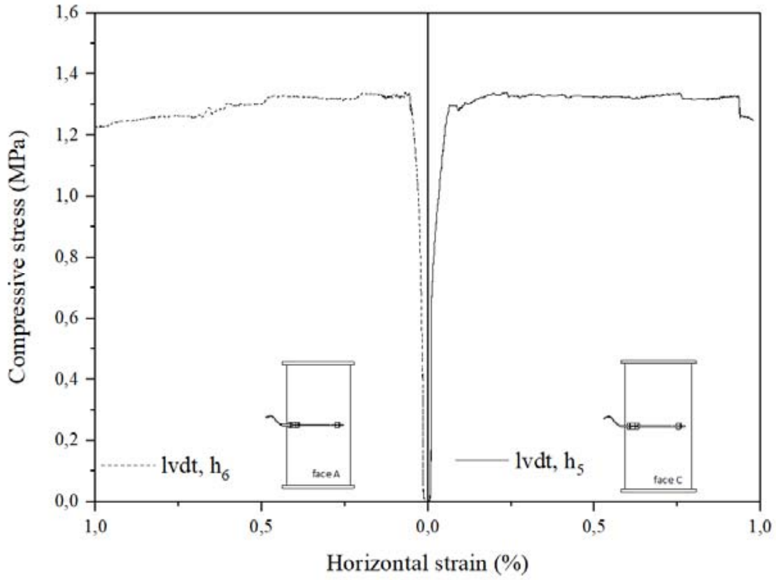

(a)

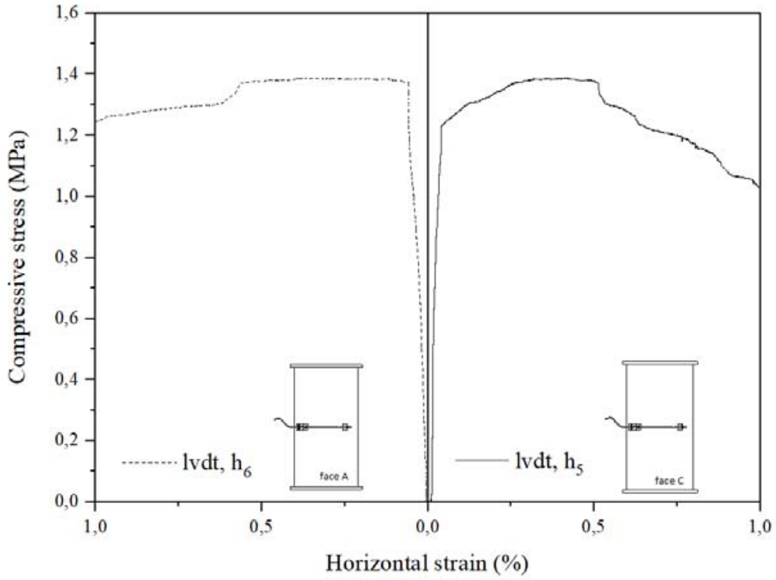

(b)

Figure 11 – Compressive stress/horizontal strain graphs on faces A and C: (a) *P4 nR* e (b) *P5 nR*

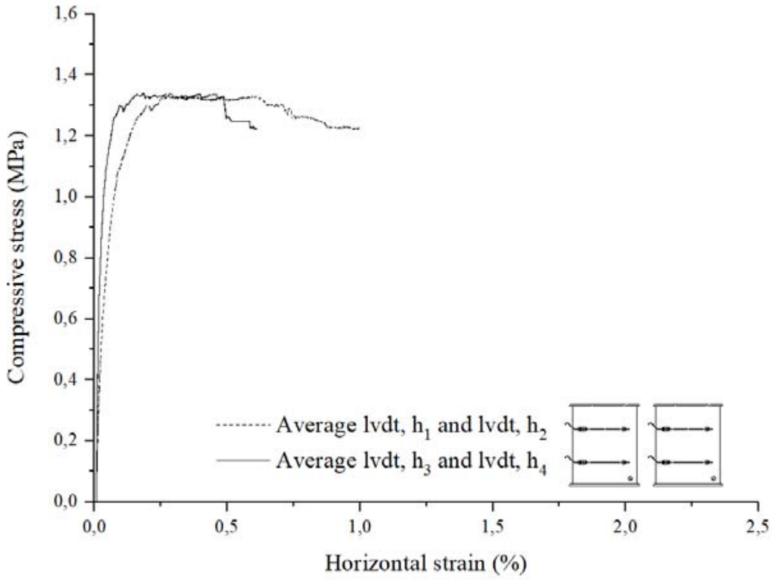

(a)

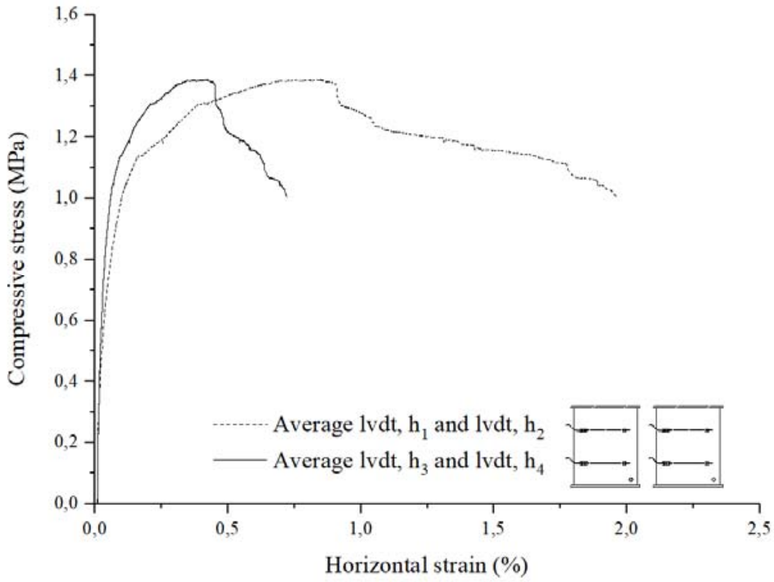

(b)

Figure 12 - Compressive stress/horizontal strain graphs on faces B and D: (a) *P4 nI* e (b) *P5 nI*

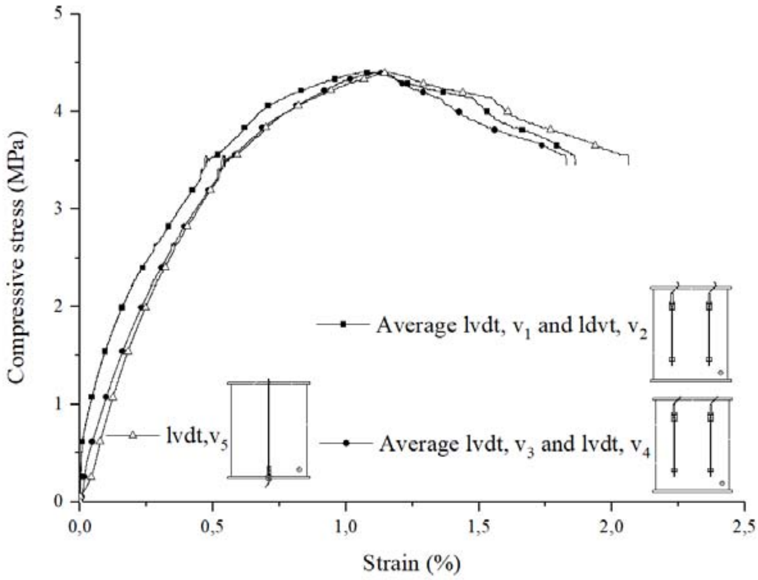

(a)

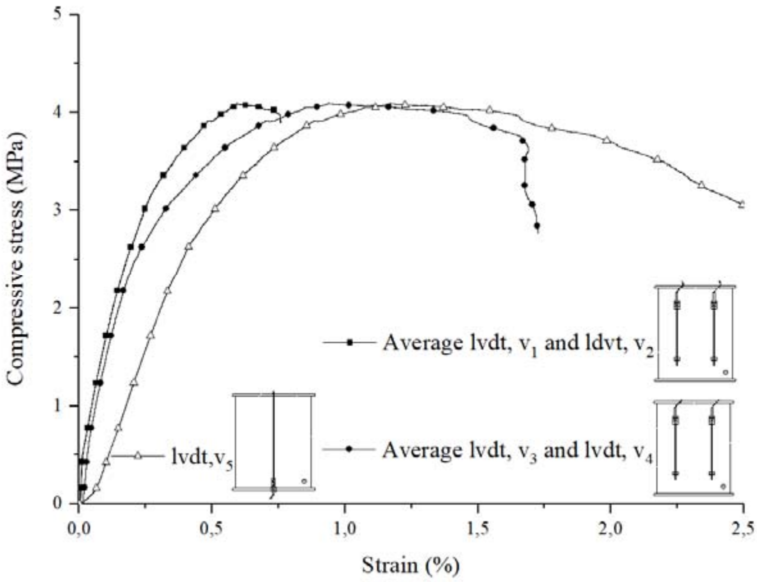

(b)

Figure 13 – Compressive stress/vertical extension graphs: (a) *P1 IB* e (b) *P3 IB*

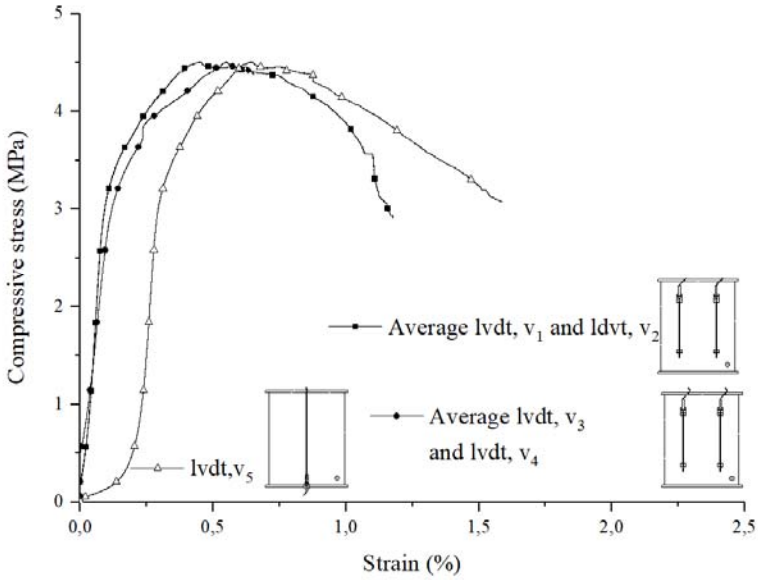

(a)

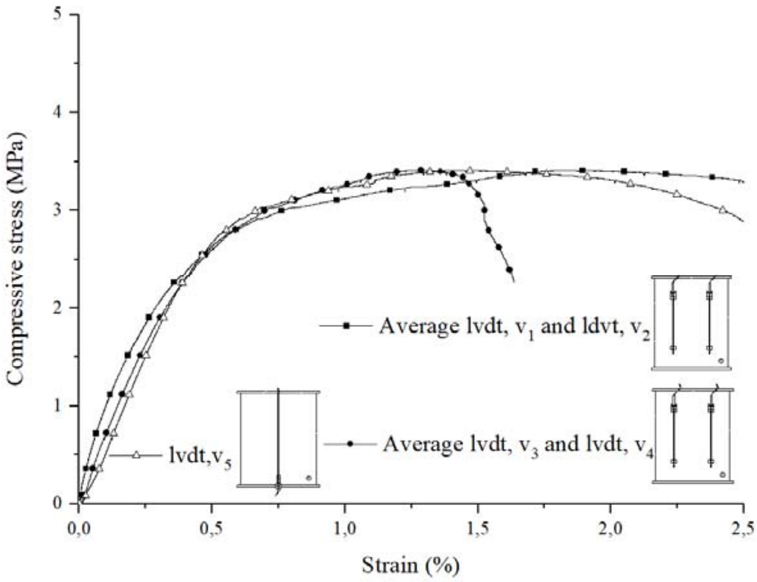

(b)

Figure 14 – Compressive stress-vertical extension graphs: (a) *P2 IA* e (b) *P6 IA*

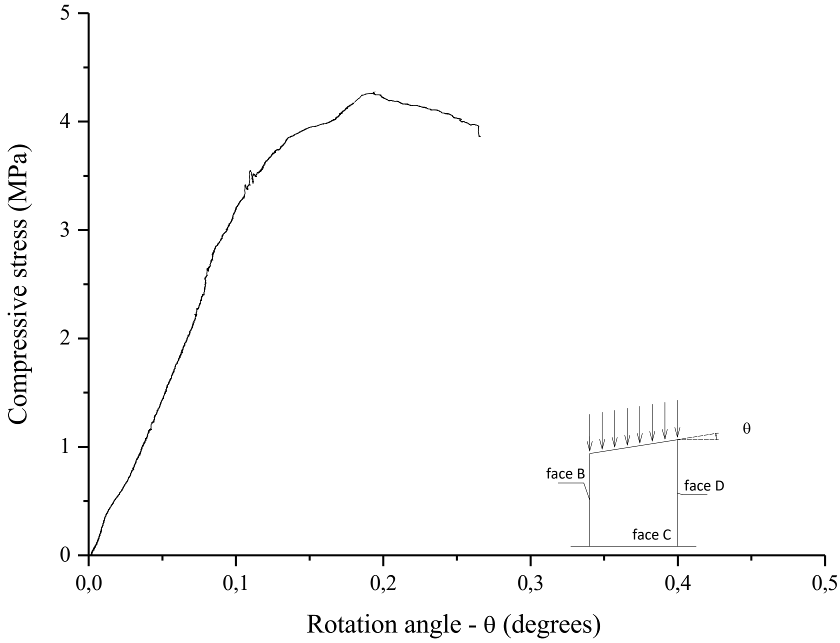

(a)

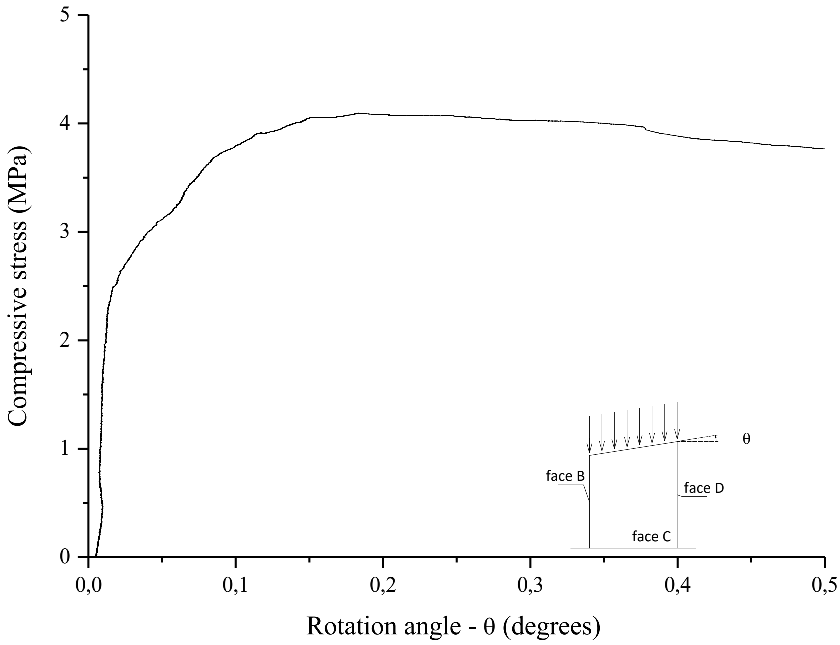

(b)

Figure 15 – Compressive stress/Rotation angle of the walls: (a) *P1 IB;* (b) *P3 IB*

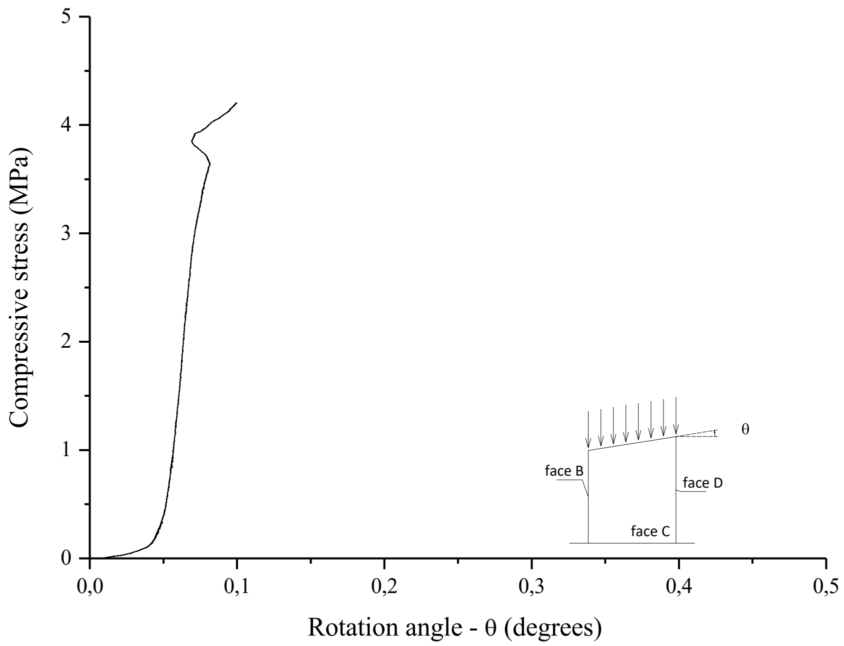

(a)

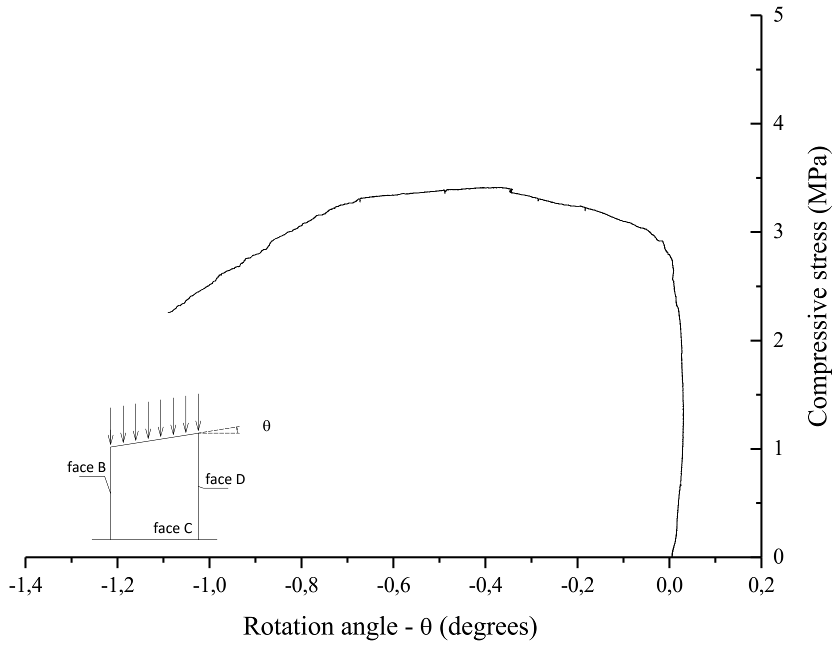

(b)

Figure 16 – Ratio compressive stress vs angle of rotation of the walls: (a) *P2 IA;* (b) *P6 IA*

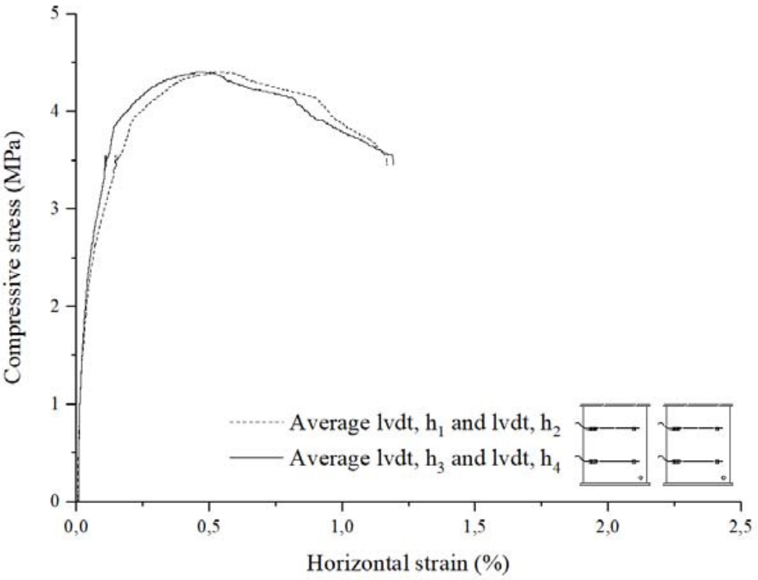

(a)

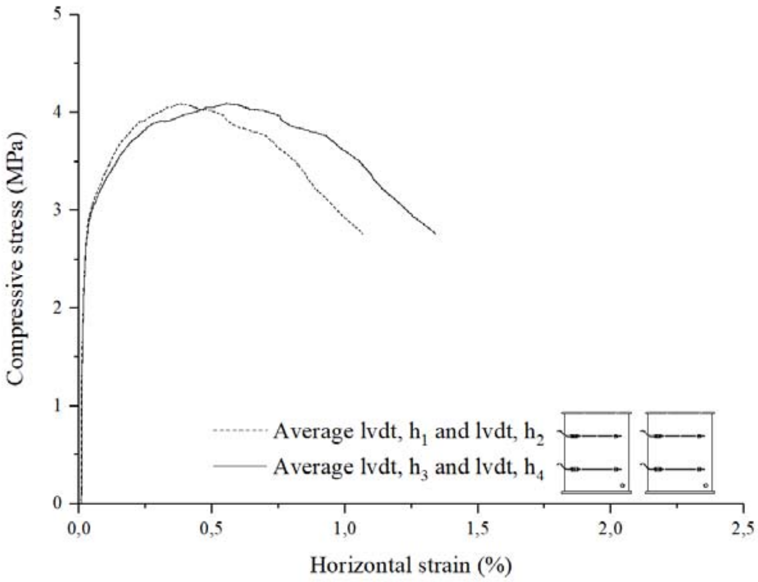

(b)

Figure 17 – Compressive stress-horizontal extension graphs: (a) *P1 IB*; (b) *P3 IB*

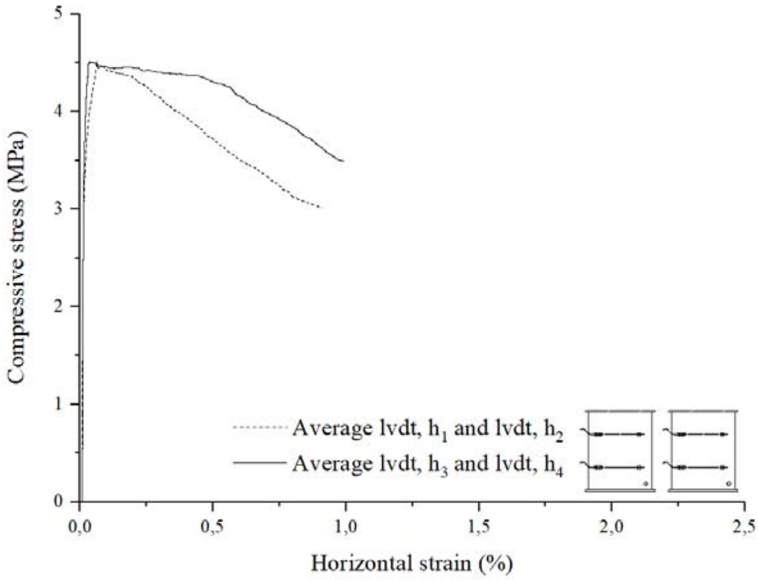

(a)

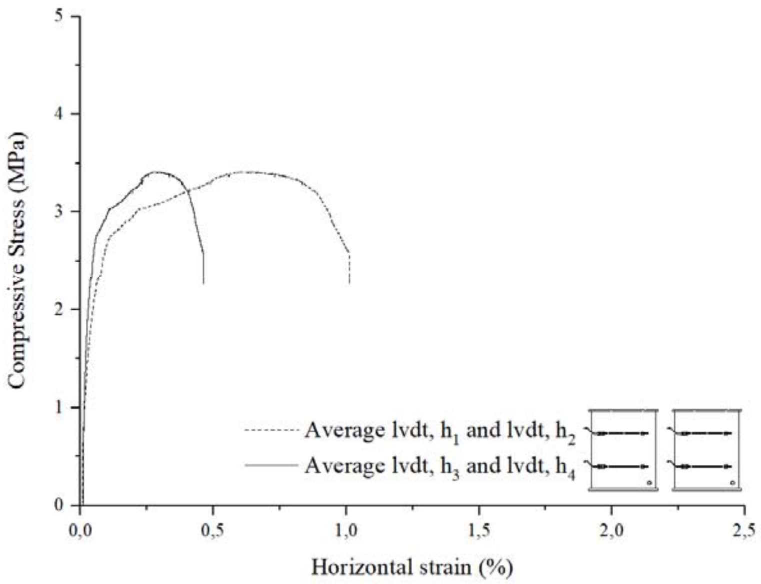

(b)

Figure 18 – Compressive stress-horizontal extension graphs: (a) *P2 IA*; (b) *P6 IA*

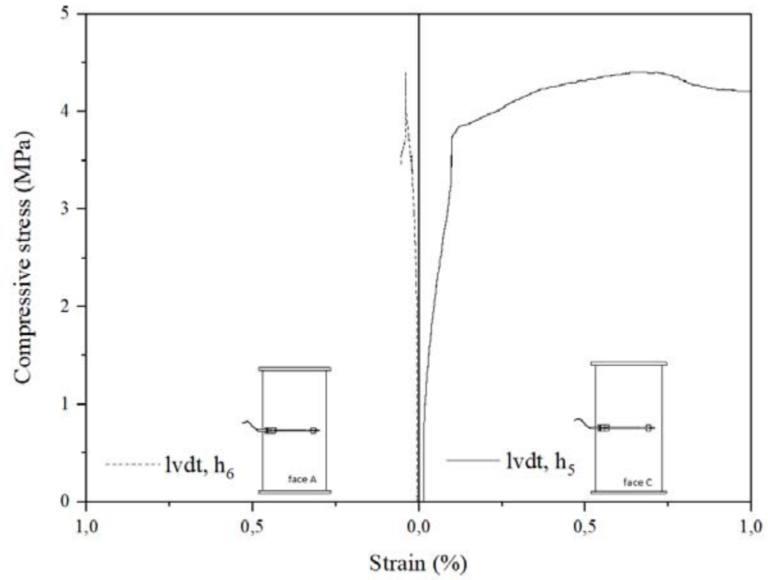

(a)

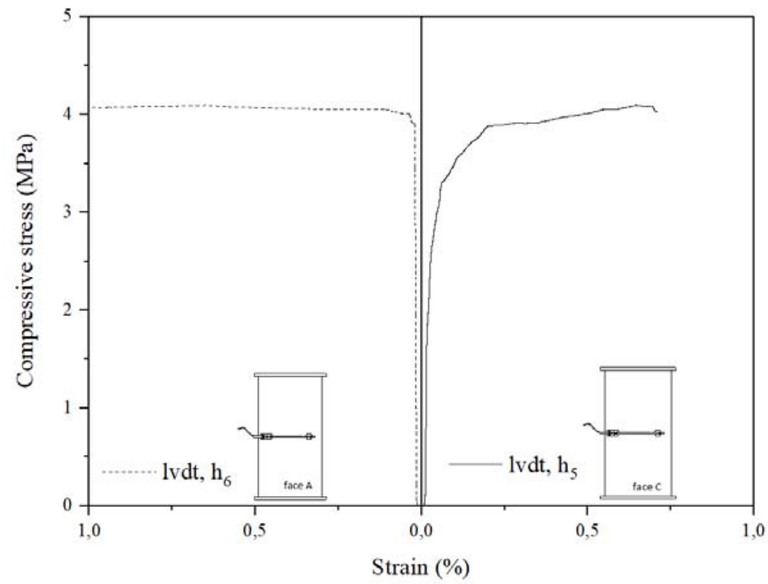

(b)

Figure 19 – Graphs compressive stress-horizontal extension on the transverse faces A and C: (a) *P1 IB* e (b) *P3 IB*

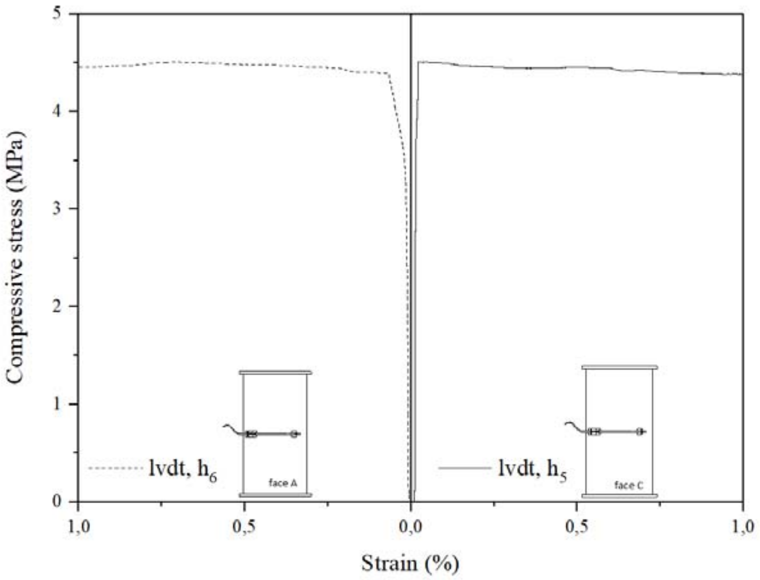

(a)

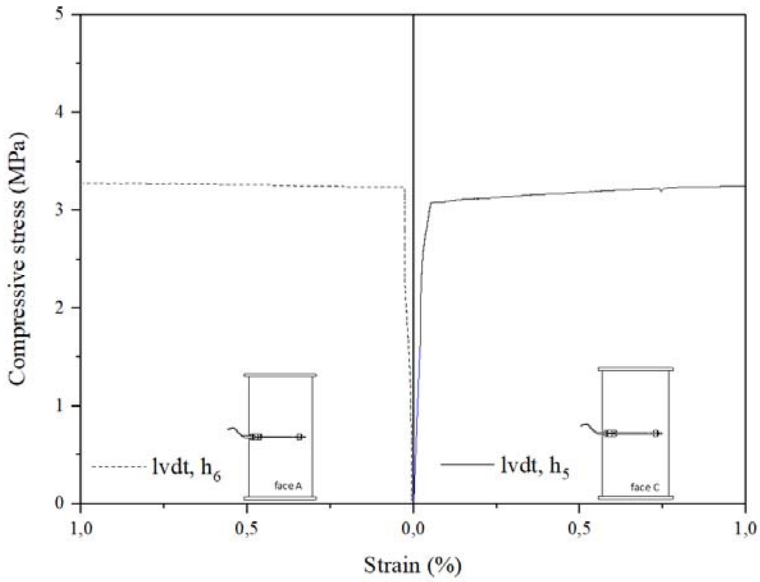

(b)

Figure 20 – Graphs compressive stress-horizontal strain on the transverse faces A and C: (a) *P2 IA* e (b) *P6 IA*

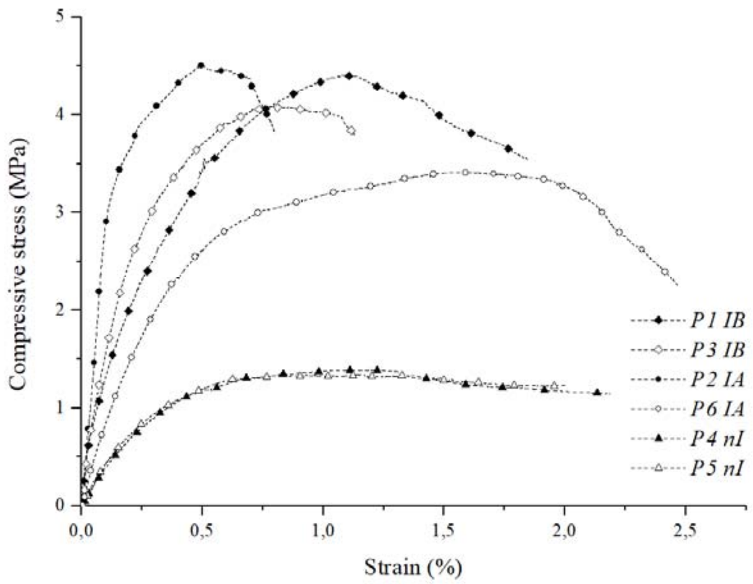

Figure 21 – Compressive stress-strain graphs for all tested walls

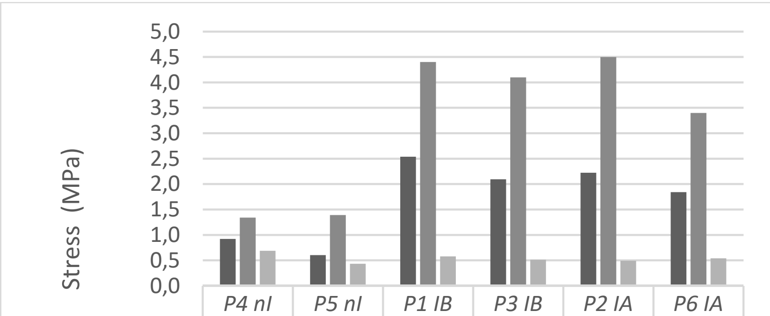

	P4 nI	P5 nI	P1 IB	P3 IB	P2 IA	P6 IA
Stress (MPa)	0,9	0,6	2,5	2,1	2,2	1,8
fc (MPa)	1,3	1,4	4,4	4,1	4,5	3,4
% fc	69%	43%	58%	51%	49%	54%

Figure 22 – Compressive stress level for which the first crack with horizontal direction appears vs. maximum compressive strength

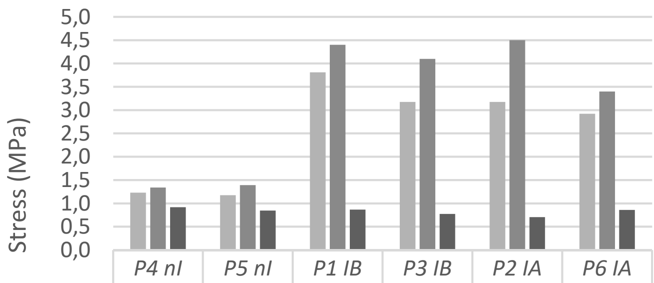

	P4 nI	P5 nI	P1 IB	P3 IB	P2 IA	P6 IA
Stress (MPa)	1,2	1,2	3,8	3,2	3,2	2,9
fc (MPa)	1,3	1,4	4,4	4,1	4,5	3,4
% fc	92%	85%	87%	77%	71%	86%

Figure 23 – Compressive stress level for which the first crack with vertical direction appears vs. maximum compressive strength

TABLES

Table 1 – Results obtained in mechanical tests. Coefficients of variation in brackets (%)

Age	Specimen	f_c (MPa)	$E_{[30\text{-}60\%]}$ (MPa)	δ_{peak} (%)	G_f (N/mm)	du (mm)
28 days	prismatic	0.71 (16.9)	-	-	-	-
90 days	prismatic	0.76 (18.2)	-	-	-	-
150 days	prismatic	0.85 (11.9)	-	-	-	-
150 days	cylinder	0.77 (13.8)	679.9 (9.1)	0.35 (24.9)	1.15 (21.4)	1.54 (31.4)

Table 2 – Main properties of the grouts A and B. Coefficients of variation (%) in brackets

	Flow Time Cone Marsh 1000mL[§] (seconds)			Bleeding[§] (in 100mL graduated cylinders)	Compressive Strength[§] at 28 days (MPa)	Flexural Strength[§] at 28 days (MPa)	Tensile Bond Strength[#] at 90 days (MPa)
	t = 0 min	t = 30min	t = 60min				
Grout A	79	105	110	0	21.4 (4.9)	4.1 (2.7)	1.26 (16.6)
Grout B	40	42	45	0	21.5 (15.2)	3.5 (10.8)	0.87 (9.5)

[§] Mean result of three tests of 160x40x40 mm^3 specimens

 # Mean result of six tests in yellow granite substrate

Table 3 – Results obtained in compression tests for non-injected masonry walls

Wall	$f_{c,w}$ (MPa)	$\varepsilon_{v,p}$ (%)	$\varepsilon_{h,p}$ (%)	E_0 (MPa)	$E_{[30\text{-}60\%]}$ (MPa)	$\nu_{[30\text{-}60\%]}$
P4 nI	1.34	0.80	0.24	513.3	296.9	0.15
P5 nI	1.39	1.17	0.64	467.3	263.0	0.21
Average	1.37	0.98	0.44	490.3	280.0	0.18

Table 4 – Summary of test results on walls injected with *grout A*

Wall	$f_{c,w}$ (MPa)	$\varepsilon_{a,p}$ (%)	$\varepsilon_{h,p}$ (%)	E_0 (MPa)	$E_{[30\text{-}60\%]}$ (MPa)	$\nu_{[30\text{-}60\%]}$
P2 IA	4,5	0,56	0,09	4272,0	2500,0	0,01
P6 IA	3,4	1,48	0,42	980,2	533,3	0,13

Average	4,0	1,02	0,26	2626,1	1516,5	0,07

Table 5 – Summary of test results on walls injected with *grout B*

Wall	$f_{c,w}$ (MPa)	$\varepsilon_{a,p}$ (%)	$\varepsilon_{h,p}$ (%)	E_0 (MPa)	$E_{[30\text{-}60\%]}$ (MPa)	$\nu_{[30\text{-}60\%]}$
P1 IB	4,4	1,08	0,48	1978,5	597,0	0,20
P3 IB	4,1	0,68	0,42	2661,1	1053,0	0,10
Average	4,3	0,88	0,45	2319,8	825,0	0,15

Table 6 – Comparison of the mean values obtained in the tests in each type of reinforced wall with the average obtained in the two non-reinforced walls

Walls	Δf_c (%)	$\Delta\varepsilon_{v,p}$ (%)	$\Delta\varepsilon_{h,p}$ (%)	ΔE_0 (%)	$\Delta E_{[30\text{-}60\%]}$ (%)
(P2 + P6) IA	+188	+4,5	-42	+410	+441
(P1 + P3) IB	+210	-10	+2	+373	+145

Table 7 - Data obtained from experimental tests of stone wall models

Authors	Injection grouts		Wall dimensions (cm)	Variation after injection (%)		
	Composition or author designation	Compressive strength at 28 days (MPa)		f_c	E	f_t
Vintzileou & Tassios (1995)	*A*	30	40x60x120	150	37 ♦	64∴
	B	13		200	50 ♦	-
Miltiadou- Fezans *et al.* (2006)	*NHL5*	2,82	45x104x120	65	20#	110
	Ternary	4,08		116	0,08#	230
	NHL5	2,82		65	-13#	120
Toumbakari (2002)	*13b-10*	6,4	40x60x120	61	125♥	0,06
	Cb-0	14,6		62	37♥	97
	13b-0	5,2		21	-30♥	107
Valluzzi (2000) Valluzzi *et al.* (2001)	*FenX-A+F*	5,10	50x80x140	46	21♣	-
	FenX-B	3,23		13	93♣	-
Silva (2008)	*Commercial Grout*	12**	30x60x110	80##	1♣	-
Almeida *et al. (*2012)	*CL+HL+S*	0,50	40x120x250*	60	40	-

** Tests on real walls, so the dimensions are approximate; ** Manufacturer data*

 # Without reference about the procedure, ## A prior state of damage was not applied. The displayed value is relative to a reference wall; ♣ Corresponding to 30-60% of the respective compressive strength; ♥ Corresponding to 30% of the respective compressive strength; ♦ Corresponding to the tangent of 1/3 of the average compressive strength; ♠ After loading-unloading cycles; ∴ Considered by the authors as $f_{wt,0}$=0,1MPa